m-Plane GaN Schottky barrier diodes fabricated with MOVPE layer on several off-angled *m*-plane GaN substrate

Atsushi Tanaka [*,1,2], Yuto Ando[3], Kentaro Nagamatsu[1], Manato Deki[1], Heajeong Cheong[1], Barry Ousmane[3], Maki Kushimoto[3], Shugo Nitta[1], Yoshio Honda[1], and Hiroshi Amano[1, 2, 4, 5]

[1] Institute of Materials and Systems for Sustainability, Nagoya University, Furo-cho, Chikusa-ku, 464-8601 Nagoya, Japan
[2] National Institute for Materials Science, 1-1, Namiki, 305-0044 Tsukuba, Japan
[3] Department of Electrical Engineering and Computer Science, Nagoya University, Furo-cho, Chikusa-ku, 464-8603 Nagoya, Japan
[4] Akasaki Research Center, Nagoya University, Furo-cho, Chikusa-ku, 464-8603 Nagoya, Japan
[5] Venture Business Laboratory, Nagoya University, Furo-cho, Chikusa-ku, 464-8603 Nagoya, Japan

Received ZZZ, revised ZZZ, accepted ZZZ
Published online ZZZ (Dates will be provided by the publisher.)

Keywords GaN, m-plane, Schottky barrier diode, facet.

In this study, GaN m-plane Schottky barrier diodes were fabricated by metalorganic vapor-phase epitaxy (MOVPE) on several off-cut angled gallium nitride (GaN) substrates and the off-cut angle dependence of impurity incorporation were investigated. We show that the MOVPE layer on the substrate inclined 5° toward the [000-1] direction has extremely low impurity incorporation. These results provide important suggestions for the fabrication of *m*-plane power devices.

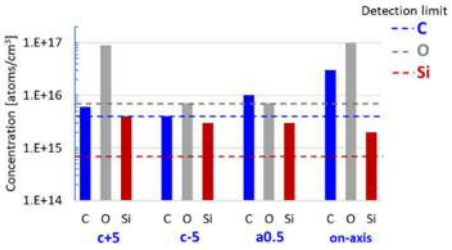

Secondary-ion mass spectrometry results for the *c*+5 sample, *c*−5 sample, *a*0.5 sample, and on-axis sample; the detection limits are indicated by the dashed lines

1 Introduction

Because of its wide band gap, high critical electric field strength, and significant bulk mobility, gallium nitride (GaN) is expected to have applications in high-performance power devices. There has been considerable interest in using the *c*-plane as the plane on which vertical power devices are fabricated [1–7], because there are many practical uses of optical applications such as light emitting diodes (LEDs) and lateral power devices such as high electron mobility transistors (HEMTs) on c-plane. However, whether the polar *c*-plane or a nonpolar plane such as the *m*-plane is more suitable for vertical power devices has not been adequately investigated. For example, the important GaN material properties with respect to the design of power devices, such as the impact ionization coefficient and the channel mobility without using a two-dimensional electron gas, should be elucidated.

We have been investigating *m*-plane GaN devices [8,9], which are less frequently investigated than *c*-plane devices. We initially studied a device with a simple structure: an *m*-plane Schottky barrier diode (SBD). We reported that an *m*-plane epitaxial layer has pyramidal hillocks and that each facet of the pyramidal hillocks has different characteristics. SBD on pyramidal hillocks has larger leakage current at the facet inclined toward [0001] than other facets of pyramidal hillocks [9].

To further investigate *m*-plane GaN devices, an epitaxial layer with a flat surface is needed. Other researchers have reported a method to obtain an *m*-plane epitaxial layer with a flat surface [10]. In the present study, we report the characteristics of *m*-plane GaN SBDs fabricated on an epilayer on several off-angled *m*-plane GaN substrates. The results lead to important

suggestions regarding the fabrication of *m*-plane GaN devices.

2 Experimental procedures

Commercially available n-type wurtzite GaN $(10\bar{1}0)$ *m*-plane substrates with off-cut angles of 5° toward the [0001] direction (*c*+5), off-cut angles of 5° toward the $[000\bar{1}]$ direction (c−5), off-cut angles of 0.5° toward the $[\bar{1}2\bar{1}0]$ direction (*a*0.5), and off-cut angles of 0.05° toward the [0001] and $[\bar{1}2\bar{1}0]$ directions (on-axis) were used in this study. A metalorganic vapor-phase epitaxy (MOVPE) layer was grown on the substrates as an unintentionally doped n^- layer of an SBD. For the MOVPE process, trimethylgallium (TMGa) and ammonia (NH_3) were used as precursors and hydrogen (H_2) was used as the carrier gas. Epitaxial layers on all substrates were grown simultaneously under a temperature of 1100°C, a pressure of 760 Torr, and V/III ratios of 1019. The target thickness was 4 μm, and the growth time was 1 h. As a cathodic ohmic contact on the backside of the sample, Ti/Al/Ti/Au (30/100/20/150 nm) metal layers were deposited by electron-beam evaporation followed by a rapid thermal annealing process at 650°C for 5 min under ambient N_2 conditions. In addition, an anode was fabricated using Ni/Au (20/150 nm) metal layers, which were deposited using electron-beam evaporation as Schottky contacts with a diameter of 500 μm on the surface of the MOVPE layers (figure 1).

The surface morphology of the MOVPE layers was observed using differential interference contrast (DIC) microscopy, white interference microscopy, and atomic force microscopy (AFM). Current density–voltage (*J*–*V*) and capacitance–voltage (*C*–*V*) characteristics of the SBDs were measured using a semiconductor parameter analyzer and a capacitance meter, respectively. Secondary-ion mass spectrometry (SIMS) was conducted to measure the concentrations of unintentional impurities incorporated during the epitaxy process.

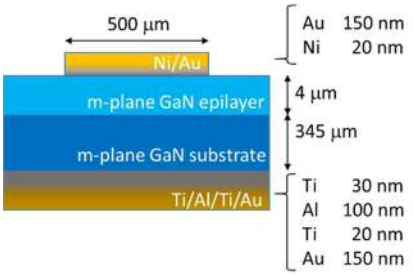

Figure 1 Schematic of a Schottky barrier diode.

3 Experimental results

Figure 2 presents overall views of the MOVPE layer surface morphology for each off-angled sample, as observed through DIC microscopy and AFM. As previously reported [10–14], macroscopically, a number of hillocks were observed on the on-axis samples, whereas the surface of the other samples (*c*+5, c−5, and *a*0.5) was flat, without hillocks. In the on-axis samples, microscopically, an orderly step-and-terrace structure was observed at the facet of the hillocks.

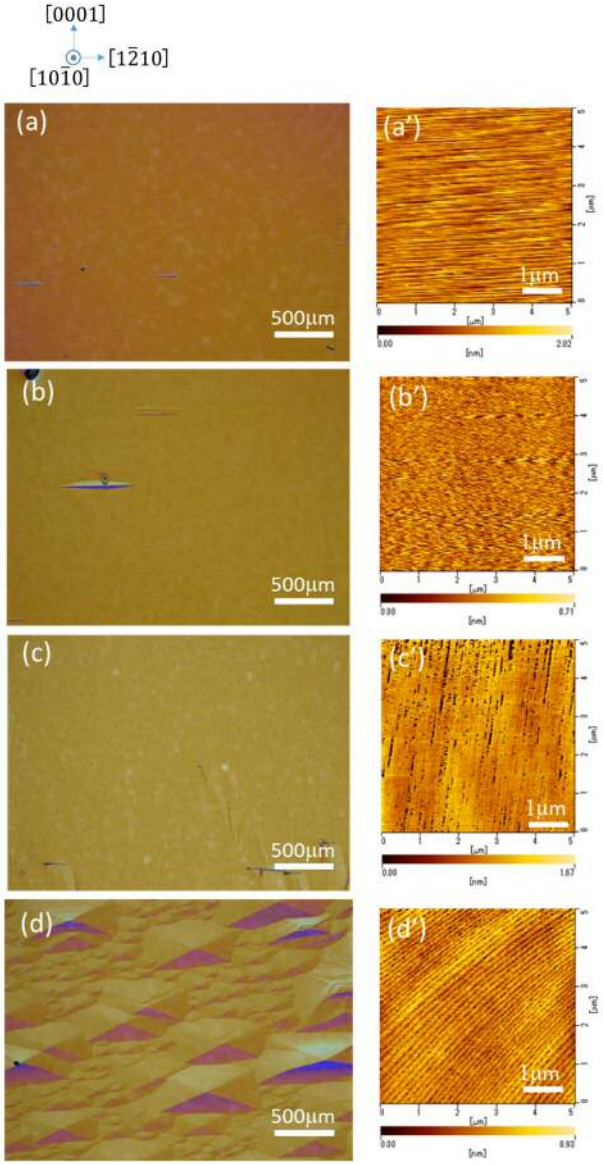

Figure 2 Differential interference contrast microscopy images and atomic force microscopy images of the *m*-plane MOVPE surface on substrates with off-cut angles of 5° toward the [0001] direction (a) (a′), 5° toward the $[000\bar{1}]$ direction (b) (b′), 0.5° toward the $[\bar{1}2\bar{1}0]$ direction (c) (c′), and 0.05° toward the [0001] and $[\bar{1}2\bar{1}0]$ directions (d) (d′)

The arithmetic average roughness (*Ra*) and the step height of these samples are similar to those of the surface of a facet on a pyramidal hillock. Table 1 shows the measured MOVPE layer thickness determined by scanning electron microscope (SEM) and the *Ra* and step height of each sample.

Table 1 Characteristic diode values of each sample

Off angle	MOVPE layer thickness [μm]	*Ra* [nm]	Average step height [nm]
5° toward +*c*	3.8	0.35	1.0
5° toward −*c*	3.6	0.08	0.5
0.5° toward *a*	3.9	0.40	1.6
on-axis	4.6	0.10	0.6

Figure 3 demonstrates typical *J–V* characteristics of SBDs fabricated on the MOVPE layer on each off-cut angled substrate. The sample on the *c*+5 substrate exhibits SBD characteristics. The samples on the *c*−5 and *a*0.5 substrates show insulator-like characteristics. The sample with an on-axis substrate shows leaky diode characteristics.

Figure 4 shows the effective donor concentration profiles derived from the *C–V* characteristics. The diode samples on the *c*+5 and the on-axis substrates exhibit diode *J–V* characteristics. The Nd–Na concentration is approximately 5×10^{16} [cm^{-3}]. For the samples with *c*−5 and *a*0.5 substrates, because the effective donor concentrations are quite low, the depletion layers are elongated over the MOVPE layer even at low bias. Therefore, the effective donor concentration in the MOVPE layer could not be measured.

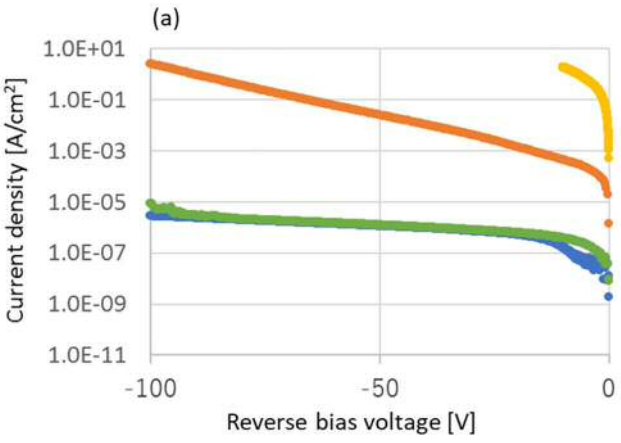

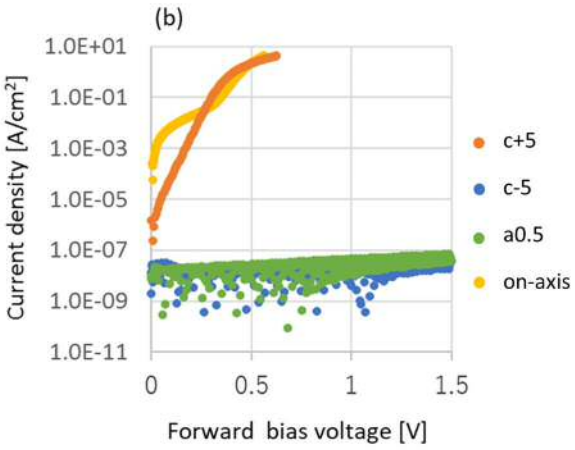

Figure 3 *J–V* characteristics of the Schottky barrier diodes fabricated on the MOVPE layer on each off-cut angled substrate: (a) reverse-biased characteristics and (b) forward -biased characteristics

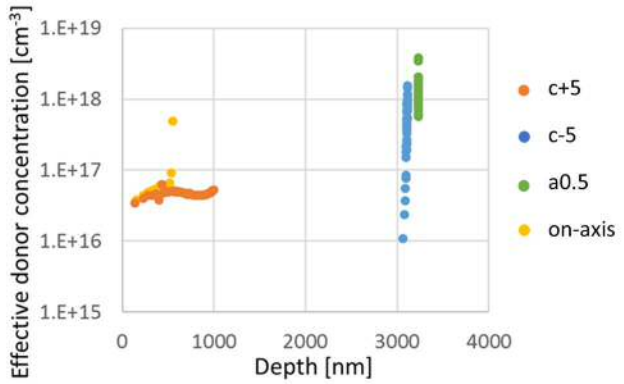

Figure 4 Effective donor concentration depth profiles derived from the *C–V* characteristics of SBDs on substrates with different off-cut angles

Except for the sample with an on-axis substrate having a surface structure such as facets with several characteristics and apexes of hillocks at the Schottky contact interface, these effective donor concentration results are consistent with the *J–V* characteristics. The Schottky barrier height ϕ_B and the *n* factor were obtained as 0.72 eV and 1.07, respectively, from the *J–V* curve for the sample with a *c*+5 substrate; these results are characteristic of a diode. The *J–V* and *C–V* characteristics of the MOVPE layer on the *c*−5 and *a*0.5 substrates exhibit intrinsic insulator-like characteristics. ϕ_B was simply calculated using the following equation [4],

$$\phi_{B(I-V)} \qquad \frac{A^* T^2}{J_0}\Big), \; A^* = \frac{4\pi e m^* k^2}{h^3}, \qquad (1)$$

where k and h are the Boltzmann constant and Planck constant, respectively. T is temperature, e is the elec-

tron charge, and A* is the effective Richardson constant. Using the electron effective mass of n-GaN m* = 0.20m_0 [15], A* was calculated to be 24.0 $Acm^{-2}K^{-2}$. J_0 was determined by performing a curve fit on the *J*–*V* curves using the equation

$$J = J_0 \left[\exp\left(\frac{eV}{nkT}\right) - 1 \right], \quad (2)$$

where V is the applied voltage, and n is the ideality factor.

To confirm the origin of the donor, each MOVPE layer on the off-cut angled substrates was analyzed by SIMS. Figures 5(a), 5(b), 5(c), and 5(d) present the SIMS results for the samples with *c*+5, *c*−5, *a*0.5, and on-axis substrates, respectively. Figure 5(a) shows that the *c*+5 substrate more easily incorporated oxygen from the chamber environment during MOVPE growth compared with the other off-cut angled substrates. In the case of the effective donor concentration profile of the sample with a *c*+5 substrate, approximately half of the incorporated oxygen appears to function as an active as donor in the MOVPE layer. Figure 5(b) indicates that impurity incorporation from the environment during MOVPE growth on a c−5 substrate is extremely small; an ideal undoped epilayer was obtained. This ideal epilayer is responsible for the insulator-like structure of the SBD with a *c*−5 substrate. In figure 5(c), which corresponds to the sample with an *a*0.5 substrate, although the carbon concentration is slightly higher, similar to the c−5 sample, impurity incorporation is also very low. The carbon, oxygen, and silicon detection limits of the secondary-ion mass spectrometer are 4×10^{15} [atoms/cm^3], 7×10^{15} [atoms/cm^3], and 7×10^{14} [atoms/cm^3], respectively. Figure 6 shows the detection limit of each impurity and the impurity concentration of each sample. In the *c*−5 sample, the concentrations of the carbon and the oxygen are below the detection limit. Thus, the MOVPE layer on a *c*−5 substrate is an ideal undoped epilayer with a very low impurity concentration. Figure 5(d) shows the results for the sample with an on-axis substrate. In this case, the SIMS measurement area was selected to include a pyramidal hillock apex at its center to obtain impurity data from the four facets of the pyramidal hillocks. A pyramidal hillock has four facets: one facet inclined toward [0001], one facet inclined toward $[000\bar{1}]$, and two facets inclined toward $<\bar{1}2\bar{1}0>$. The SIMS profile of the on-axis sample comprises the features of the SIMS profiles of the samples. The profile of oxygen, which was mostly present at the interface between the substrate and the MOVPE layer and decreased toward the surface, is similar to the profile of oxygen in the *c*+5 sample (figure. 5(a)). The carbon profile shows a flat concentration over the entire MOVPE layer, similar to the carbon profile of the *a*0.5 sample (figure. 5(c)). Thus, with respect to the incorporation of the fewest impurities, the MOVPE layer on the three off-cut angled substrates (*c*+5, *c*−5, and *a*0.5) are considered to have the same properties as each facet of the pyramidal hillocks of the MOVPE layer on the on-axis substrate. That is, three kinds of stable facets—the facet inclined toward $[000\bar{1}]$, the facet inclined toward $[000\bar{1}]$, and facets inclined toward $[\bar{1}2\bar{1}0]$—appear in the *m*-plane MOVPE. In the case of the off-cut angled substrates, we can separately fabricate each type of facet.

(a) c+5

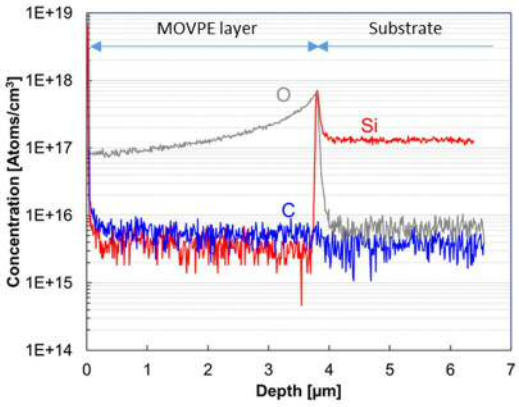

(b) c-5

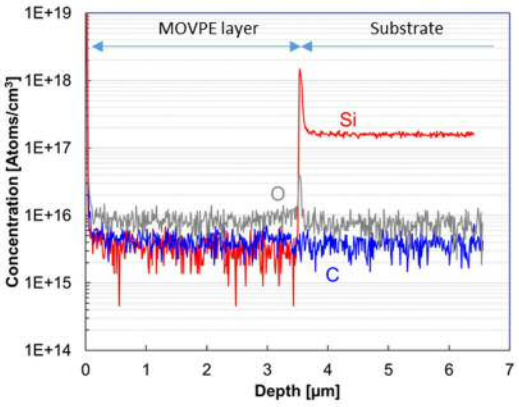

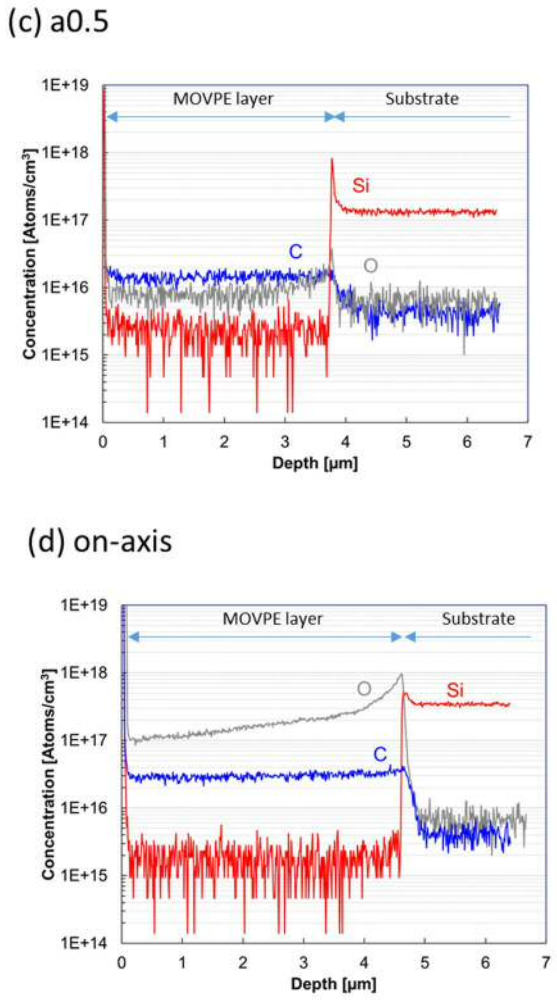

Figure 5 Secondary-ion mass spectrometry results for the (a) *c*+5 sample, (b) *c*−5 sample, (c) *a*0.5 sample, and (d) on-axis sample

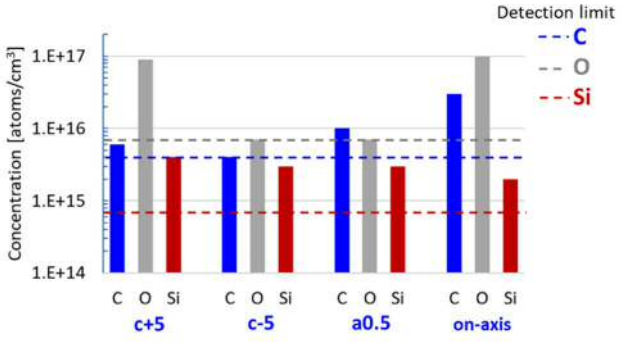

Figure 6 Secondary-ion mass spectrometry results for the *c*+5 sample, *c*−5 sample, *a*0.5 sample, and on-axis sample; the detection limits are indicated by the dashed lines

4 Discussion

In the case of *c*-plane crystal growth of GaN, researchers have reported that the incorporation of oxygen into Ga faces is difficult, whereas oxygen is easily incorporated into N faces [16]. However, in the case of *m*-plane crystal growth of GaN, the *c*−5 sample is considered to have a stepped N face, whereas the *m*-plane terrace exhibits difficulty incorporating oxygen. To investigate this difference, we observed the cross sections of samples by SEM. Figure 7(a) shows an SEM image of the cross section of a sample fabricated using a longer MOVPE time to clearly reveal the facets on a *c*−5 substrate. Facets tilted 27° from the *m*-plane toward the $[000\bar{1}]$ direction are observed at the surface of the MOVPE layer. The schematic in Figure. 7(b) shows the atomic arrangement of a $(10\bar{1}\bar{1})$ Ga-rich face tilted 28° from the *m*-plane. If a facet tilted 27° from a Ga-rich *m*-plane is $(10\bar{1}\bar{1})$ facet and the growing edge, then the incorporation of oxygen is difficult [17]. On the *c*+5 sample, facets tilted 14° from the *m*-plane toward the [0001] direction are observed at the surface of the MOVPE layer as shown in figure 7(c). If this facet is $(20\bar{2}1)$ and the growing edge then it is considerable that the incorporation of oxygen is easy, similar to the case of $(000\bar{1})$ growth and $(10\bar{1}1)$ growth. In the a0.5 samples, such a considerable facet was not observed. For strict and further understanding, detailed investigations of surface reconstruction and surface band bending are necessary.

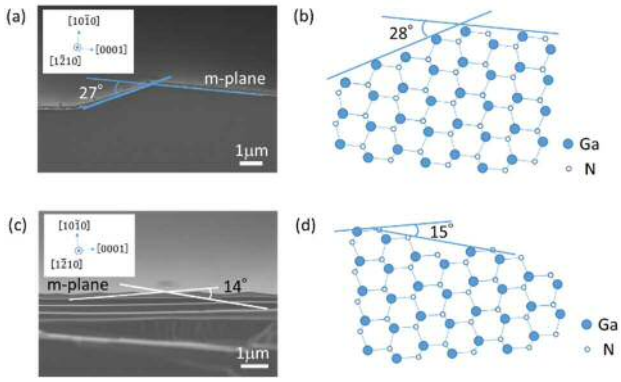

Figure 7 (a) Cross-sectional SEM image and (b) a schematic crystal structure of the MOVPE layer on a *c*−5 substrate and (c) Cross-sectional SEM image and (d) a schematic crystal structure of the MOVPE layer on a *c*+5 substrate

5 Conclusion

Herein, we reported the substrate off-cut angle dependence of *m*-plane GaN SBD characteristics of samples fabricated on MOVPE layers. We found that the *m*-plane MOVPE layers on different off-cut angled substrates exhibit different impurity uptakes. To our

knowledge, these differences have not been previously reported. Finally, we found that the MOVPE layer on a substrate inclined 5° toward the [000$\bar{1}$] direction exhibits extremely low impurity incorporation. These findings are important for the fabrication of power devices capable of withstanding high voltages.

Acknowledgements Part of this work is supported by the Cross-ministerial Strategic Innovation Promotion Program.

References

[1] G. T. Dang, A. P. Zhang, F. Ren, X. A. Cao, S. J. Pearton, H. Cho, J. Han, J. I. Chyi, C. M. Lee, C. C. Chuo, S. N. George Chu, and R. G. Wilson, IEEE Trans. Electron Devices **47**, 692 (2000).

[2] Y. Yoshizumi, S. Hashimoto, T. Tanabe, and M. Kiyama, J. Cryst. Growth **298**, 875 (2007).

[3] K. Matocha, T. P. Chow, and R. J. Gutmann, IEEE Trans. Electron Devices **52**, 6 (2005)..

[4] J. Suda, K. Yamaji, Y. Hayashi, T. Kimoto, K. Shimoyama, H. Namita, and S. Nagao, Appl. Phys. Exp., **3**, 101003 (2010)

[5] Z. Hu, K. Nomoto, B. Song, M. Zhu, M. Qi, M. , X. Gao, V. Protasenko, D. Jena, and H. G. Xing, Appl. Phys. Lett., **107**, 243501 (2015).

[6] M. Qi, K. Nomoto, M. Zhu, Z. Hu, Y. Zhao, V. Protasenko, B. Song, G. Li, J. Verma, S. Bader, P. Fay, H. G. Xing, and D. Jena, Appl. Phys. Lett., **107**, 232101 (2015).

[7] T. Oikawa, Y. Saijo, S. Kato, T. Mishima, and T. Nakamura, Nucl. INSTRUMENTS METHODS Phys., **365**, 168 (2015).

[8] O. I. Barry, A. Tanaka, K. Nagamatsu, S. Bae, K. Lekhal, J. Matsushita, M. Deki, S. Nitta, Y. Honda, and H. Amano, J. Cryst. Growth, **468**, 552 (2017).

[9] A. Tanaka, K. Nagamatsu, J. Matsushita, M. Deki, Y. Ando, M. Kushimoto, S. Nitta, Y. Honda, and H. Amano, Phys. Status Solidi A, **214,** 1600829 (2017).

[10] A. Hirai, Z. Jia, M. C. Schmidt, R. M. Farrell, S. P. Denbaars, S. Nakamura, and J. S. Speck, Appl. Phys. Lett., **91**, 191906 (2007).

[11] R. M. Farrell, D. A. Haeger, X. Chen, C. S. Gallinat, R. W. Davis, M. Cornish, K. Fujito, S. Keller, S. P. Denbaars, S. Nakamura, and J. S. Speck, Appl. Phys. Lett., **96**, 2319070 (2010).

[12] C. Q. Chen, M. E. Gaevski, W. H. Sun, E. Kuokstis, J. P. Zhang, R. S. W. Fareed, H. M. Wang, J. W. Yang, G. Simin, M. A. Khan, H.P. Maruska, D. W. Hill, Mitch M. C. Chou, and B. Chai, Appl. Phys. Lett., **81**, 3194 (2002)

[13] M. Rudzinski, R. Kudrawiec, L. Janicki, J. Serafinczuk, R. Kucharski, M. Zajac, J. Misiewicz, R. Doradzinski, R. Dwilinski, and W. Strupinski, J. Cryst. Growth, **328**, 5 (2011).

[14] K. M. Kelchner, L. Y. Kuritzky, S. Nakamura, S. P. Denbaars, and J. S. Speck, J. Cryst. Growth, **411**, 56 (2015).

[15] A. S. Barker and M. Ilegems, Phys. Rev. B **7**, 743 (1973)

[16] N. A. Fichtenbaum, T. E. Mates, S. Keller, S. P. Denbaars, and U. K. Mishra, J. Cryst. Growth, **310**, 1124 (2008).

[17] S. C. Cruz, S. Keller, T. E. Mates, U. K. Mishra, and S. P. Denbaars, J. Cryst. Growth, **311**, 3817 (2009).